# BEAM DYNAMICS STUDIES ON THE ISAC-II POST-ACCELERATOR AT TRIUMF

M. Pasini, R.E. Laxdal, TRIUMF, Vancouver, Canada
P.N. Ostroumov, Argonne National Lab, USA

## Abstract

The TRIUMF/ISAC facility, now a world leader in rare isotope production and acceleration, is constructing ISAC-II [1, 2], that will allow the acceleration of ion beams with $3 \leq A/q \leq 7$ to an energy of at least 6.5 MeV/u for masses up to 150. The upgrade will include the addition of a superconducting heavy-ion linac delivering an effective voltage of 43 MV. The first order design of the new transfer lines and post-accelerator have been optimized to provide simultaneous acceleration of several charge states (multicharge). The quarter wave resonators providing the acceleration have inherent rf electric and magnetic asymmetric components that complicate multi-charge acceleration and can lead to transverse emittance growth. In particular we report the realistic field simulations of the medium beta section of the SC-DTL for multi-charge acceleration.

## 1 INTRODUCTION

A first stage of ISAC-II installation will see a transfer line constructed from the ISAC-I DTL exit to join the medium-beta section of the ISAC-II SC linac for acceleration of lighter ions, $A \leq 60$, to energies above the Coulomb barrier. A schematic of the ISAC-II linear accelerator complex is shown in Fig. 1. The building for ISAC-II is now under construction with beam delivery from the first stage due in 2005.

A comprehensive first order design study[3], now complete, set the parameters of the floor layout prior to building construction. The solution includes all transport beamlines, including the first stage transfer line and second stage 90° isopath bend section[4] as well as the first order dynamics of the super-conducting linac. Designs are compatible with multi-charge acceleration to preserve beam intensity and/or allow the possibility of a second optional stripping stage to boost the final ion energy. A two-gap quarter wave
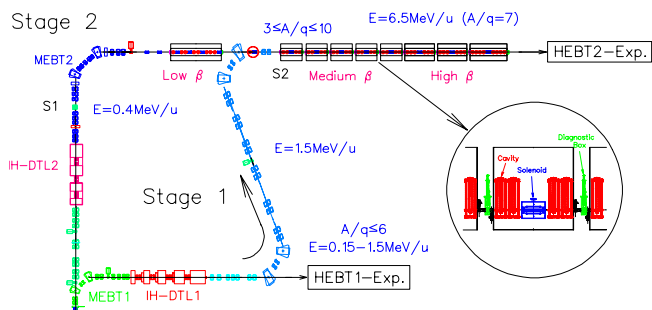


Figure 1: A schematic for the ISAC-II linac with Stage 1 and Stage 2 installations complete.

bulk niobium structure[5] is chosen for ISAC-II with three cavity geometries corresponding to low, medium and high $\beta_o$ (4.2%, 7.2%, 10.5%) values and rf frequencies of 70.7, 106.08 and 141.4 MHz respectively. Design gradients are set at 5 MV/m for the low beta cavities and 6 MV/m for the medium and high beta sections. The large gradients produce proportionally larger defocussing and steering fields and together with multicharge acceleration pose new challenges for heavy ion linac design.

## 2 BEAM SIMULATION CODES

The envelope codes TRACE-3D and COSY-$\infty$ have been used to design transfer lines and optimize linac lattice parameters. The Monte-Carlo code LANA has been used to set the first order specifications of linac parameters assuming standard cavity field approximations. Electromagnetic fields created with HFSS and CST-MWS are then installed in LANA and TRACK to study 'realistic' acceleration dynamics. TRACK is also used to study the effect of misalignments of linac components.

## 3 STAGE 1 BEAM DYNAMICS

Detailed beam dynamics simulations have concentrated on Stage 1 with five, four cavity medium beta cryomodules and two six cavity high beta cryomodules. A single superconducting solenoid is positioned at the center of each cryomodule for transverse focussing with diagnostic boxes positioned between cryomodules at waists in the transverse envelopes (Fig. 1). Solenoids provide a larger transverse acceptance than quadrupoles for transporting beams with multiple charge states[6].

### 3.1 First Order Simulations

The simulations include all transport from the output of the ISAC DTL to the end of the 7-module ISAC-II SC linac for two single charge cases corresponding to ions with $A/q$ of 3 and 6 and for a multicharge case with reference ion $_{132}Sn^{31+}$ with five charge states, $Q = 29, ...33$, accelerated through the SC linac simultaneously. The lattice easily accommodates the rf defocussing from the high gradient cavities (Fig. 2(a)). The longitudinal emittance is broadened as each charge revolves around a different synchronous phase. The transverse emittance increase is $\leq 5\%$.

### 3.2 Realistic Field Dynamics

Realistic field studies are complete for the 10.5 m long medium beta section consisting of five cryomodules with four cavities and one 35 cm long superconducting solenoid in each. Two main asymmetries in the medium beta cavity fields are responsible for differences between the 'simple
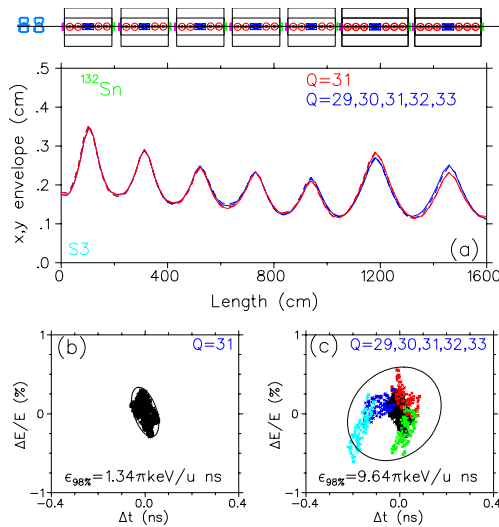
Figure 2: Transverse beam envelopes and final longitudinal phase space ensembles for both a single charge state, $_{132}Sn^{31+}$ (20% of the beam), and multiple charge states, $_{132}Sn^{29+,...,33+}$ (80% of the beam) after acceleration through the SC-DTL linac (Stage 1) to 8.3 MeV/u. Initial beam emittances are 0.2$\pi$mm-mr and 1.2$\pi$keV/u-ns.

cavity model' and 'realistic field' simulations. Inherent in quarter wave cavities are both a vertical electric dipole field and a radial magnetic field that give velocity and phase dependent vertical kicks to the beam[7]. The vertical steering produced by the cavity shifts the beam off-center and can lead to loss of dynamic aperture and phase dependent transverse emittance growth especially for multi-charge beams. The steering can be largely cancelled by displacing the cavity vertically so the electric focussing field compensates for the magnetic kick[8].

The cylindrical stem produces a quadrupole asymmetry in the transverse rf electric fields. The asymmetry leads to a mismatch between horizontal and vertical motion. The degree of mismatch is dependent on the magnitude of the asymmetry and on the relative strength of the defocussing rf with respect to the focussing optics in the lattice cell. In a quadrupole lattice the two planes are independent and different match conditions can be used to eliminate emittance growth. In a solenoidal lattice the two planes are rotated periodically and a mismatch between transverse planes can lead to transverse emittance growth once the beam is delivered to a quadrupole transport system.

**Cavity and Linac Variants**  Three cavity models, shown in Fig. 3, are used to study the effect of the quadrupole asymmetry. The *nominal* case simulates the prototype medium beta ($\beta_o$ = 0.072) cavity; 40 mm gap, 20 mm bore, and a cylindrical inner conductor of ID=60 mm. In the *flat* model the inner conductor is squeezed to 40 mm in the beam direction and the grounded beam ports are extended to maintain the original gap. This lowers the design $\beta_o$ to ~0.06. In the *donut* model cylindrical half tubes are welded to the flattened inner conductor
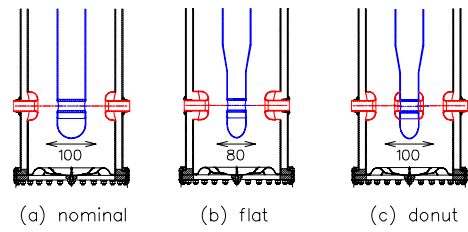


Figure 3: Three different cavity geometries considered in quadrupole asymmetry study.

to maintain the gap with a design $\beta_o$ of the original.

The field asymmetries from the three models are summarized in Fig. 4 over the operating velocity range required of the cavity for an accelerating gradient of 6 MV/m, an ion of $A/q = 3$, and a phase of $\phi_s = -30°$. Shown are the uncorrected and corrected vertical steering components and the vertical and horizontal defocussing perturbations for a 1 mm displacement from the electrical axis. The dipole steering components can be reduced to less than 0.1 mrad over the whole velocity range, for even the lightest beams, by shifting the cavities down by 0.8 mm in the *nominal* and *donut* cases and 0.6 mm in the *flat* case with respect to the beam and solenoid axis.

Simulations are done for three standard medium beta linacs; (a) the *NOMINAL* with twenty *nominal* cavities, (b) *FLAT8* with eight *flat* cavities and twelve *nominal* cavities and (c) *DONUT* with twenty *donut* cavities. Case (c) represents a linac with the same velocity profile as (a) but negligible quadrupole asymmetry while (b) is a practical
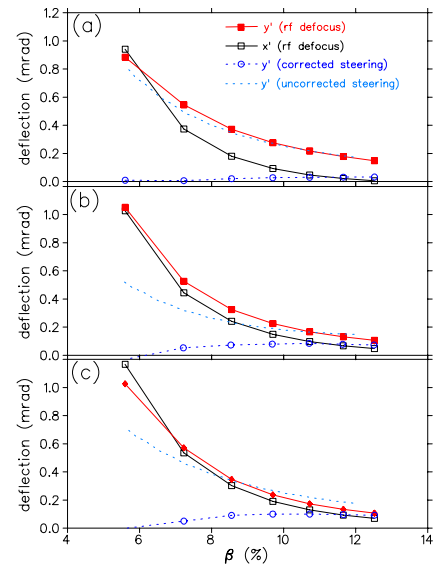


Figure 4: Focussing and steering perturbations for the three cavity geometries (a) *nominal* (b) *flat* (c) *donut* as calculated in HFSS. Shown are the uncorrected and corrected vertical steering components (dashed lines) and the vertical and horizontal defocussing perturbations for a 1 mm displacement from the electrical axis.
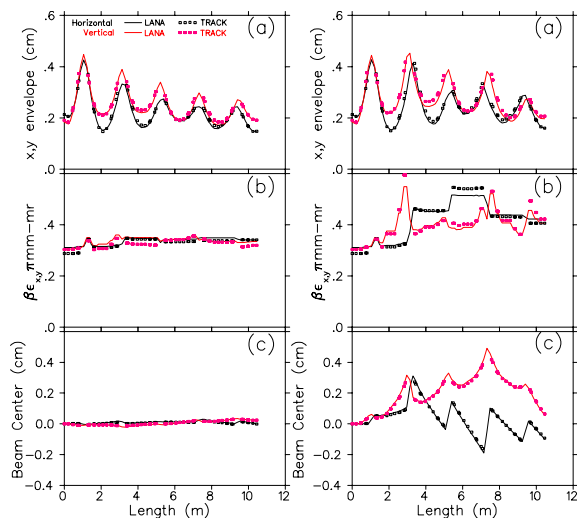
Figure 5: Beam envelopes (a), transverse emittances (b) and beam centroids (c) are given for the *NOMINAL* medium beta section assuming $A = 30$ with charge states $Q = 9, 10, 11$ for cavities displaced 0.8 mm (left series) and undisplaced cavities (right series). Initial beam emittance is $\beta\epsilon_{x,y} = 0.3\pi$mm-mr and $1.5\pi$kev/u-ns.

alternative to the base design where lower $\beta$ cavities with reduced quadrupole asymmetry are substituted where the rf defocussing is relatively more acute.

**Beam Steering** Beam envelopes, transverse emittances and beam centroids are given in Fig. 5 for the twenty cavity *NOMINAL* linac assuming $A = 30$ with charge states $Q = 9, 10, 11$ for displaced cavities (left series) and undisplaced cavities (right series). The steering correction increases the dynamic aperture and reduces transverse emittance growth. LANA and TRACK results are shown for comparison and agree well.

**Quadrupole Asymmetry** The quadrupole asymmetry inherent in the *nominal* cavity is responsible for the splitting of the $x$ and $y$ beam envelopes in Fig. 5(a). Calculations show that the small transverse emittance growth is due mostly to phase dependent coupling and only slightly to the quadrupole asymmetry for a matched aligned beam with design normalized emittance of $0.3\pi$ mm-mrad and longitudinal emittance $1.5\pi$keV/u-ns. The sensitivity of the cavity/lattice to mismatch and misalignment is tested with a single charge species beam with $\epsilon_z = 12\pi$keV/u-ns and $\beta\epsilon_{x,y} = 1.2\pi$mm-mrad (each $\sim 10\times$ expected emittances). Beam envelopes and transverse emittances for an $A/q = 3$ beam are given for the three linac variants in Fig. 6. Results suggest that for light beams an improvement in dynamic aperture can be gained by substituting some *flat* cavities at the beginning of the medium beta section. Completely eliminating the quadrupole asymmetry as in *DONUT* does improve the mismatch between $x$ and $y$ but without the improvement in transverse beam quality. Further, simulations show that as the mass to charge ratio of
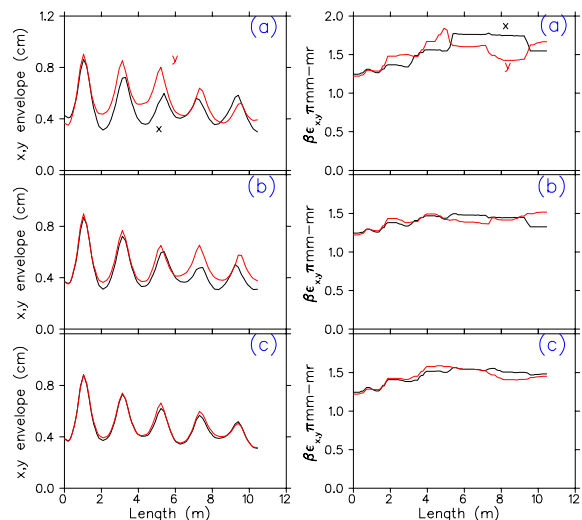


Figure 6: Beam envelopes and transverse emittances for large test beams ($\epsilon_z = 12\pi$keV/u-ns, $\beta\epsilon_{x,y} = 1.2\pi$mm-mrad) of $A/q = 3$ through the three medium beta cryomodule variants (a) *NOMINAL* (b) *FLAT8* (c) *DONUT*.

the ion increases, the quadrupole asymmetry becomes less important since the relative rf defocussing strength in the periodic cell, hence the degree of $x,y$ mismatch, is reduced compared to the focussing in the cell. Likewise, increasing the focussing in the cell by adding more solenoids will reduce the impact of the quadrupolar rf defocussing.

## 4  ACKNOWLEDGMENTS

## 5  REFERENCES

[1] R.E. Laxdal, 'Completion and Operations of ISAC-I and Extension to ISAC-II', PAC2001, Chicago, June 2001.

[2] R.E. Laxdal, 'Superconducting RF at TRIUMF/ISAC: Present Status and Future Plans', SCRF2001, Tskuba, Japan, Sept. 2001.

[3] R.E. Laxdal, M. Pasini, 'ISAC-II Optics Specifications' TRIUMF Design Note, www.triumf.ca/download/lax/ISAC5.ps.

[4] M. Pasini, R.E. Laxdal, 'An Isopath Achromatic Bending Section for Multi-charge Transport at ISAC-II', these proceedings.

[5] A. Facco, et al., 'The Superconducting Medium $\beta$ Prototype for Radioactive Beam Acceleration at TRIUMF', PAC2001, Chicago, June 2001.

[6] R. E. Laxdal, 'Progress in the Conceptual Design of the ISAC-II Linac at TRIUMF', PAC2001, Chicago, June 2001.

[7] A. Facco, 'Study on Beam Steering in Intermediate-$\beta$ Superconducting Quarter Wave Resonators', PAC2001, Chicago, June 2001.

[8] P.N. Ostroumov, K.W. Shepard, 'Correction of Beam Steering Effects in Low Velocity Superconducting Quarter-Wave Cavities', Phys. Rev. ST. Accel. Beams 11, 030101 (2001).